Journal of Studies in Science and Engineering

EngiScience Publisher

Research Article

Control and Energy Management of a Hybrid Fuel Cell and Super-Capacitors System by Combining the Backstepping Approach and the Flatness Concept

Ahmed Moutabir [1,*], Adil Barra [1], Mohamed Rafik [2], Abderrahmane Ouchatti [1]

[1] GEITIIL Laboratory, Faculty of Science Ain Chock, Hassan II University of Casablanca, Casablanca, 5366, Morocco

[2] ENSET Mohammedia, EEIS Laboratory, Hassan II University of Casablanca, Casablanca, 5366, Morocco

*Corresponding Author: Ahmed Moutabir, E-mail: a.moutabir65@gmail.com

Article Info

Article History

Received Apr 24, 2024

Revised Oct 04, 2024

Accepted Oct 08, 2024

Keywords

Hybrid System

Fuel cell

Energy Management

Super-Capacitors

Backstepping

Flatness concept

Control Strategies

Abstract

In remote and hard-to-reach areas, such as mountainous regions, the construction and maintenance of power lines are costly. As a result, an autonomous energy production system is necessary, favoring the use of renewable energies like solar panels and wind turbines. The diversification of these sources has led to their integration with an energy production grid, supplemented by storage devices and a generator to mitigate power outages. Replacing the diesel generator with a fuel cell system can ensure complete autonomy of the energy supply. The fuel cell system meets electricity demands when sunlight or wind conditions are insufficient. This paper focuses on power management in a dual-source hybrid system comprising a fuel cell and super-capacitors (SC). The first step involves modeling the fuel cell and the system's various converters. The second step includes synthesising non-linear control strategies based on the backstepping approach and energy management using the flatness concept. These strategies account for the fuel cell's dynamics and constraints. Finally, the results were validated through simulations using Matlab's SimPower tool.

1. Introduction

The urgency of addressing energy and environmental challenges has accelerated the development of renewable energy technologies. Integrating these technologies with conventional energy sources has driven advancements in various industrial sectors, particularly in stationary energy production.

Hydrogen fuel cells stand out as a green and environmentally friendly energy source [1, 2]. They operate by converting chemical energy directly into electrical energy through hydrogen oxidation, bypassing intermediate thermal or mechanical processes [3]. This results in highly efficient, scalable, and silent devices that power everything from portable electronics to vehicles and large power grids.

The unique characteristics and behaviour of fuel cells, influenced by various operational parameters, have spurred significant research and interest [4]. This research has led to several modelling methods for

fuel cells [5]. Among the different types of fuel cells, the Proton Exchange Membrane Fuel Cell (PEMFC) [6] and the Solid Oxide Fuel Cell (SOFC) [7, 8] are the most commonly used. Our study focuses on the PEMFC due to its wide power range, high efficiency, and cost-effectiveness.

Electricity generation is increasingly focused on renewable energies due to their technical and economic advantages, particularly in decentralised systems. The high costs of building and maintaining power lines make renewable energy solutions even more appealing in remote and hard-to-access locations like mountains, islands, and deserts. In these areas, autonomous energy production systems become crucial. These systems often incorporate solar panels and wind turbines to harness locally available renewable resources [9, 10]. They typically include storage devices and backup generators to ensure a continuous power supply and address potential interruptions.

A fuel cell system can replace a diesel generator to achieve total energy autonomy. This system ensures electricity is available when renewable sources like sunlight and wind are insufficient. During periods of excess energy, the surplus is used to produce hydrogen through electrolysis, which is then stored and used by the fuel cell system when needed. This setup is part of a hybrid energy grid that combines renewable photovoltaic and wind power sources, as illustrated in Figure 1.

In applications requiring high voltage from the fuel cell, two approaches are commonly used: employing a high-duty-cycle step-up converter or implementing cascaded converters. Within this hybrid system, a boost converter is used with the fuel cell to handle high voltage requirements, while a buck-boost converter manages voltage from the super-capacitors. This configuration ensures compatibility and efficient energy management across different sources [11-13].

Several types of controllers have been developed to control the various static converters used. Linear control methods such as Proportional-Integral (PI) control and approximation methods using Lyapunov's first law are still employed for non-linear systems and provide acceptable results regarding stability conditions. However, the pursuit of higher performance has led to the adoption of non-linear control strategies. At this level, notable approaches include the backstepping approach [14], sliding mode control [15], and passivity-based control [16].

Flatness is often employed to manage power in hybrid systems, as it can meet the desired objectives. A flatness concept has usually been used to manage power in hybrid systems [17-19], as it can meet the desired objectives.

In the literature, research has been conducted on Energy Management Systems (EMSs) that incorporate hybrid setups combining Fuel Cells (FCs) and Super-capacitors (SCs). These studies explore how integrating these different energy storage technologies can enhance efficiency, optimise performance, and lower costs across various applications, such as electric vehicles, renewable energy systems, and grid stability.

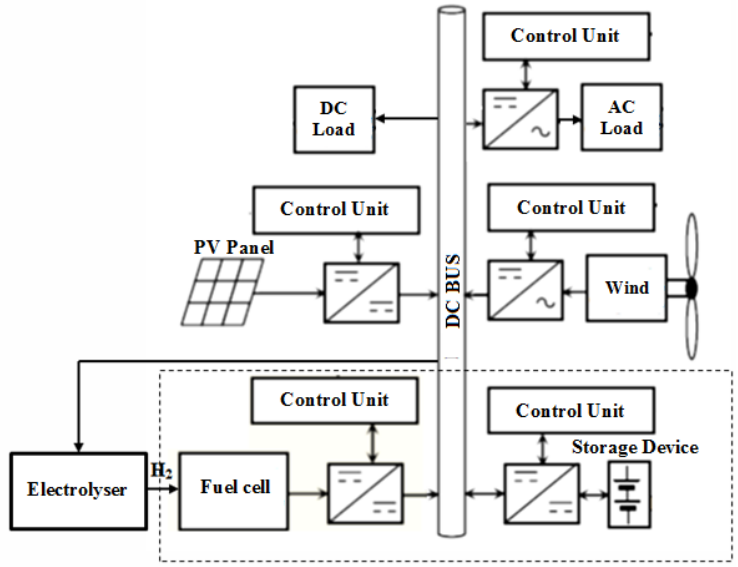

Figure 1. Autonomous hybrid system

Siangsanoh, et al. [20] proposed an architecture where the closed-loop control systems utilise an indirect-sliding mode approach for managing the inner current loop alongside energy control for the outer loop. The indirect-sliding mode technique ensures robust current regulation by creating a sliding surface to which the system state converges, while the outer loop optimises energy management and system efficiency. This combined strategy aims to enhance precision and performance in the system's operation.

In Ghavidel and Mousavi-G [21] study, a robust observer-based control method stabilises the DC-bus's voltage and ensures optimal energy source performance (FC and SC). Additionally, a fuzzy algorithm is proposed for managing the Energy Management System (EMS) of the Hybrid Energy Storage System (HESS).

Tian, et al. [22] introduced an Adaptive Neuro-Fuzzy Inference System (ANFIS) for efficiently managing power distribution between fuel cells (FCs) and batteries, commonly used in electric vehicles (EVs). The ANFIS approach integrates neural networks and fuzzy logic to control the power flow adaptively, ensuring optimal performance and efficiency in the energy management of EVs.

Li, et al. [23] investigate reinforcement learning (RL) for optimising energy management in fuel cell hybrid systems. The study introduces the challenges and potential benefits of applying RL to such systems. It then models the components of the hybrid system, including fuel cells and energy storage units. Furthermore, implementing RL algorithms is detailed, focusing on dynamically managing energy distribution and storage to enhance system efficiency and performance.

Moreover, a hybrid power management approach is proposed by Mounica and Obulesu [24] that combines an Adaptive Neuro-Fuzzy Inference System (ANFIS) with the Equivalent Consumption Minimization Strategy (ECMS). This method leverages artificial intelligence (AI) to optimise power distribution among energy sources. By integrating ANFIS and ECMS, the approach aims to enhance the

efficiency and effectiveness of power management in systems with multiple energy sources.

Recently, metaheuristic optimisation algorithms have emerged as a promising approach to improving the performance of energy management systems (EMS). Djerioui, et al. [25] propose a strategy using the Grey Wolf Optimizer (GWO) to manage energy in a hybrid fuel cell (FC) and super-capacitor (SC) system for electric vehicles (EVs). The main goal of this approach is to extend the fuel cell's lifespan by minimising harmful transient currents.

Rezk et al. [26] also present a comparative analysis of various energy management strategies for hybrid renewable energy systems (RES) involving FCs, SCs, and batteries. This study contrasts traditional methods with metaheuristic approaches, specifically the Mine Blast Algorithm (MBA) and the Salp Swarm Algorithm (SSA), to evaluate their effectiveness in managing energy.

In this work, the backstepping approach and flatness concept have been combined respectively to control the inner loop of the system and manage the power flows.

Integrating differential flatness with the backstepping approach provides a more refined and efficient control design, resulting in smoother operation and reduced chattering compared to sliding mode control. This makes it particularly advantageous for managing complex systems like hybrid power sources where precise and stable performance is crucial.

On the other hand, compared to fuzzy logic control, the proposed method provides a more precise and systematic approach for the control design, with better handling of nonlinearities, formal stability guarantees, and optimised performance. In contrast, fuzzy logic control offers flexibility and intuition but lacks the same level of formal rigour and optimisation, making the former more advantageous for complex hybrid systems requiring high precision and stability.

Finally, while differential flatness with backstepping provides structured, guaranteed control solutions, optimisation algorithms offer adaptability and versatility but may lack formal stability assurances.

The paper is structured as follows: the first section introduces the topic, while the second section details the models for the system components, including the fuel cell and converters. The third section focuses on developing various control strategies employed in the system. In the fourth section, the performance of these control strategies is demonstrated through numerical simulations conducted with Matlab/Simulink, followed by a discussion of the results.

2. Materials and Methods

2.1. System Modeling

This section describes the hybrid system, followed by the modeling and sizing of its constituents, namely the fuel cell and the converters.

2.1.1. Hybrid System Structure

The hybrid system depicted in Figure 2 integrates a primary power source, the fuel cell, with super-capacitors as storage components. The two-converter architecture is advantageous as it allows for independent control of the converters and the energy flows they manage.

- DC-DC Interleaved Boost Converter: Connected to the fuel cell, this non-reversible converter reduces the current ripple.
- DC-DC Buck-Boost Converter: Linked to the super-capacitors, this reversible converter facilitates both the storage and the release of energy.

This configuration provides several benefits, including enhanced efficiency by adjusting the voltage and current, dynamic energy management that enables quick responses to changes in energy demand, increased component lifespan through optimised operation, straightforward integration of new energy sources or storage systems, and reduced energy losses, thereby minimising losses during conversion.

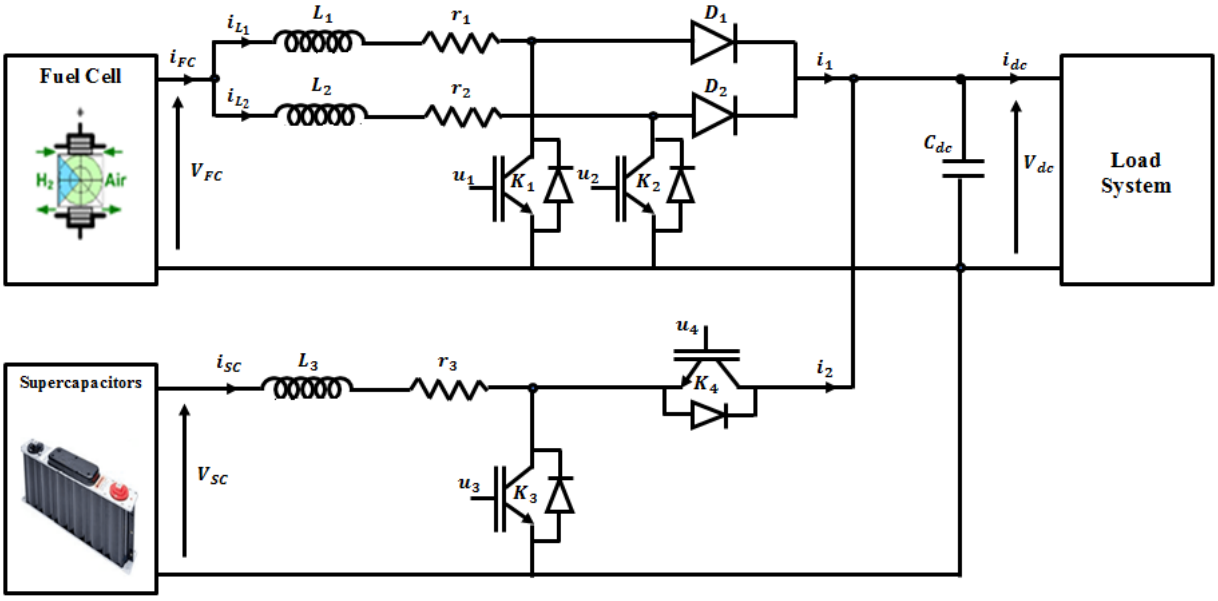

Figure 2. Hybrid system

2.1.2. Fuel Cell Model

The Proton Exchange Membrane fuel cell (PEMFC) is an electrochemical converter. It is composed of two electrodes called an anode and a cathode. The following basic chemical reactions in the anode and cathode (oxidation and reduction) describe the behaviour of the fuel cell.

$$\begin{cases} H_2 \rightarrow 2H^+ + 2e^- \\ \frac{1}{2}O_2 + 2H^+ + 2e^- \rightarrow H_2O \end{cases} \quad (1)$$

Globally, the electrochemical operation principle of a PEM fuel cell is described by the following chemical reaction:

$$H_2 + \frac{1}{2} O_2 \rightarrow H_2O \quad (2)$$

- The PEMFC (Proton Exchange Membrane Fuel Cell) model is fundamentally based on the electrochemical reactions that convert chemical energy into electrical energy. This model is typically divided into two main components:
- The Fluidic Model focuses on the behaviour of gases and fluids within the fuel cell, including their flow and interactions. It helps to understand how reactants (such as hydrogen and oxygen) are transported through the fuel cell and how water and heat are managed.

The Electrical Model describes the electrical aspects of the fuel cell, including the generation of electrical power from the electrochemical reactions and the cell's internal resistance.

The thermal model is not the primary focus here since the PEMFC operates as a heat pump at low temperatures. For simplicity, we assume a uniform temperature across the fuel cell, neglecting the complexities associated with thermal variations.

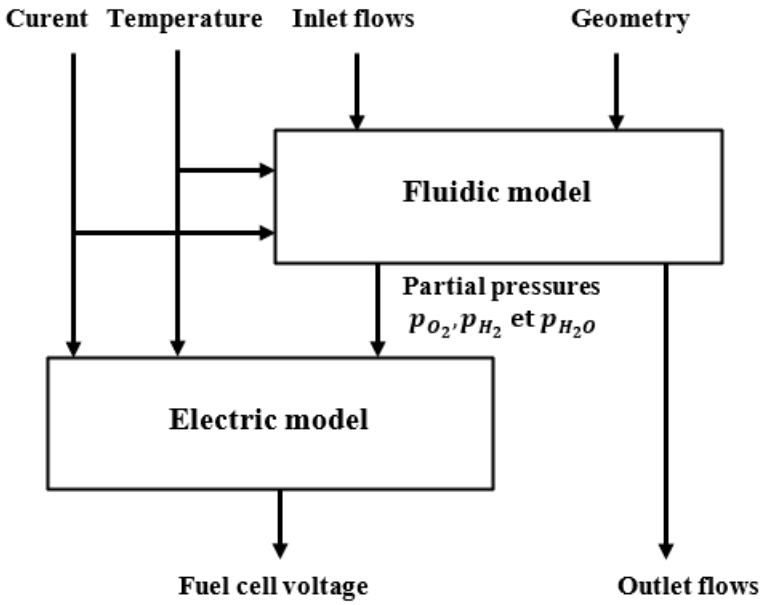

Figure 3. Block diagram of a PEMFC model

To establish the electrical model of the PEMFC, we will follow the approach described by the following descriptive diagram of the energies involved:

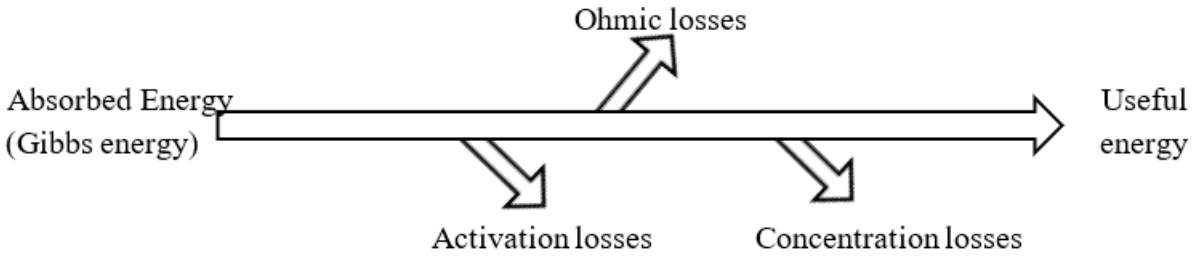

Figure 4. PEMFC energy balance

The output voltage of a Proton Exchange Membrane Fuel Cell (PEMFC), which represents the useful electrical energy generated by the cell, can be expressed as follows [26]:

$$V_{cell} = E_{Nernst} - \sum losses = E_{Nernst} - V_{act} - V_{ohm} - V_{conc} \quad (3)$$

where E_{Nernst}, V_{act}, V_{ohm} and V_{conc} represent the open cell voltage, the activation potential, the ohmic potential, and the concentration potential.

$$V_{cell} = E_{Nernst} - \left[\xi_1 + \xi_2.T + \xi_3.T.ln(C_{O_2}) + \xi_4\, ln(i_{cell})\right] - [i_{cell}.(R_M + R_C)] - [-B.ln(1 - J/J_{max})] \quad (4)$$

Where:

$$E_{Nernst} = 1{,}229 - 0{,}85.10^{-3}.(T - 298{,}15) + 4{,}31.10^{-5}.T.\left[ln(P_{H_2}) + \frac{1}{2}ln(P_{O_2})\right] \quad (5)$$

The parametric coefficients ξ_1, ξ_2, ξ_3 and ξ_4 are derived from experimental data, with their values identified and calculated in [26].

Using Matlab software, the PEM fuel cell model has been simulated with the set of parameter values depicted in Table 1. The Voltage-Current (V-I) and Power-Current (P-I) characteristics are shown in Figure 5.

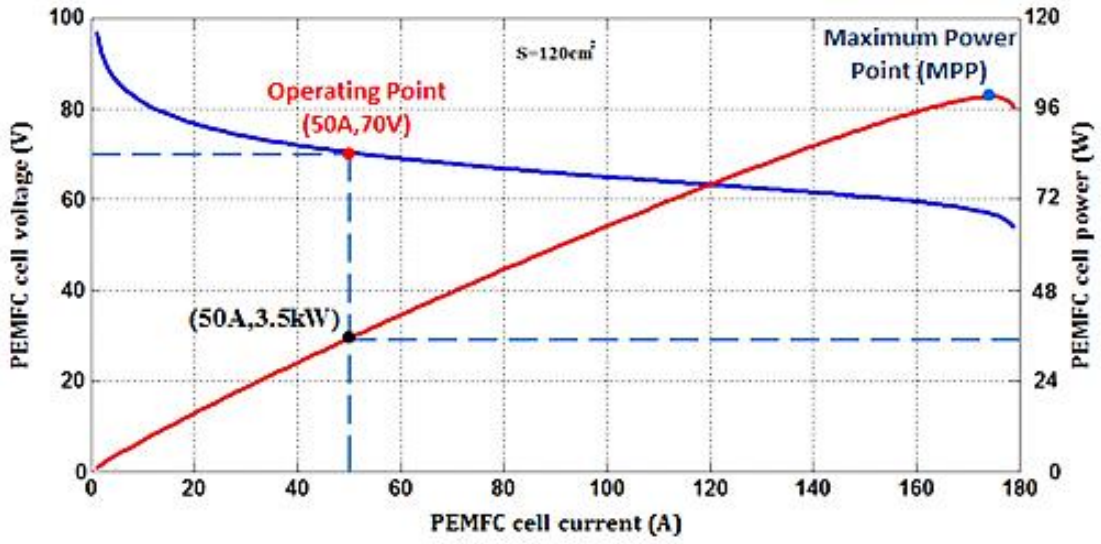

Figure 5. Fuel cell Voltage-Current (V-I) and Power-Current (P-I) characteristics

The operating point of the fuel cell is selected to optimise efficiency. It is positioned within the linear region of the Voltage-Current characteristic curve, avoiding the maximum power point where losses are significant. This choice helps minimise inefficiencies and maximise overall performance.

To optimise the use of the fuel cell, its power must satisfy the following conditions:

$$P_{FCmin} \leq P_{FC} \leq P_{FCmax} \quad (6)$$

This condition must be required by software describing the evolution of the fuel cell current and delivering its reference value.

The flowchart in Figure 6 represents the algorithm for delivering the fuel cell reference current as a function of the output power demand. The range of power variations guarantees good efficiency.

Table 1. Fuel cell parameter values

Parameters	Values	Parameters	Values
Hydrogen and oxygen partial pressures: P_{H_2}, P_{O_2}	2.10^5Pa	Water contents of the membrane: ψ	23
Parametric coefficient: ξ_1	$-0{,}922$	Kelvin temperature: T	343K
Parametric coefficient: ξ_2	0,00312	Current density maximum value: J_{max}	$2A/cm^2$
Parametric coefficient: ξ_3	$-9{,}92.10^{-5}$	Activation area: A	$120cm^2$
Parametric coefficient: ξ_4	$7{,}4.10^{-5}$	Membrane and contact resistors: $R_M + R_C$	$0{,}4.10^{-4}\Omega$
Cell number: n	100	Fuel cell voltage: V_{FC}	70V
Minimum fuel cell power P_{FCmin}	2kW	Maximum fuel cell power P_{FCmax}	6kW

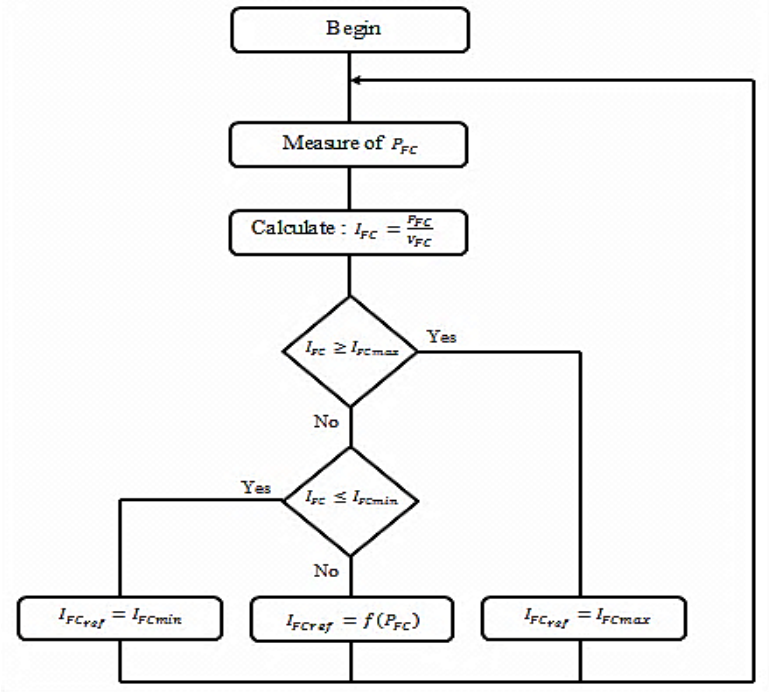

Figure 6. Flowchart determining the reference current of the Fuel cell

2.1.3. Interleaved DC-DC Boost Converter Modeling

We define the following DC-DC interleaved boost converter model by applying the Kirchhoff laws.

$$\begin{cases} \boldsymbol{i_{FC} = i_{L1} + i_{L2}} \\ \boldsymbol{L_1 \dfrac{di_{L1}}{dt} = V_{FC} - (1-\mu_1)V_{dc} - r_1 i_{L1}} \\ \boldsymbol{L_2 \dfrac{di_{L2}}{dt} = V_{FC} - (1-\mu_2)V_{dc} - r_2 i_{L2}} \\ \boldsymbol{i_1 = (1-\mu_1)i_{L1} + (1-\mu_2)i_{L2}} \end{cases} \quad (7)$$

2.1.4. DC-DC Buck-Boost Converter Modeling

For this converter, two operating modes are defined:

- Boost mode: $i_{SC} > 0$

$$\begin{cases} L_3 \dfrac{di_{SC}}{dt} = V_{SC} - r_3 i_{SC} - (1-\mu_3) V_{dc} \\ i_{2_{boost-mode}} = (1-\mu_3) i_{SC} \end{cases} \tag{8}$$

- Buck mode: $i_{SC} < 0$

$$\begin{cases} L_3 \dfrac{di_{SC}}{dt} = V_{SC} - r_3 i_{SC} - \mu_4 V_{dc} \\ i_{2_{buck-mode}} = \mu_4 i_{SC} \end{cases} \tag{9}$$

Consider a binary variable k defined by:

$$k = \begin{cases} 1 & \text{si} i_{SC} > 0 \\ 0 & \text{si} i_{SC} < 0 \end{cases}$$

The following equation expresses the global duty ratio for the Buck-Boost converter denoted μ_{34}

$$\mu_{34} = k(1-u_3) + (1-k)u_4 \tag{10}$$

Then, the Buck-Boost global model is defined by:

$$L_3 \frac{di_{SC}}{dt} = V_{SC} - \mu_{34} V_{dc} - r_3 i_{SC} \tag{11}$$

The DC bus is defined

$$C_{dc} \frac{dV_{dc}}{dt} = (1-u_1) i_1 + (1-u_2) i_2 + u_{34} i_{SC} - i_{dc} \tag{12}$$

Finally, the average model of the hybrid system is given by:

$$\begin{cases} \dot{x}_1 = -\dfrac{(1-u_1)}{L_1} x_4 - \dfrac{r_1}{L_1} x_1 + \dfrac{V_{PAC}}{L_1} \\ \dot{x}_2 = -\dfrac{(1-u_2)}{L_2} x_4 - \dfrac{r_2}{L_2} x_2 + \dfrac{V_{PAC}}{L_2} \\ \dot{x}_3 = -\dfrac{u_{34}}{L_3} x_4 - \dfrac{r_3 + r_{SC}}{L_3} x_3 + \dfrac{x_5}{L_3} \\ \dot{x}_4 = -\dfrac{(1-u_1)}{C_{dc}} x_1 - \dfrac{(1-u_2)}{C_{dc}} x_2 + \dfrac{u_{34}}{C_{dc}} x_3 - i_{dc} \\ \dot{x}_5 = -\dfrac{1}{C_{SC}} x_3 \end{cases} \tag{13}$$

- x_1, x_2, x_3, x_4et $x_5$are respectively the average values of the following quantities $i_{L1}, i_{L2}, i_{SC} V_{dc}$et v_{SC} which represent the inductance currents respectively denoted L_1,$L_2, L_3$and the DC bus voltage. To these values correspond the following references: $x_{1ref}, x_{2ref}, x_{3ref}, x_{4ref}$ and x_{5ref} which respectively represent the reference currents of the different inductances $I_{L_{1ref}}$, $I_{L_{2ref}}$, $I_{SC_{ref}}$, the bus reference voltage $V_{dcref}$and the super-capacitors reference voltage V_{SCref}.
- $u_1, u_2$and $u_{34}$are respectively the average values of the duty cycles μ_1, μ_2 et μ_{34}.

2.2. Control System Strategies

2.2.1. Control Objectives

This section aims to develop and analyse control and energy management strategies that can be able to satisfy the following objectives:

- Impose the desired power according to the proposed consumption profile.
- Ensure the global stability of the system.
- Guarantee the output voltage tracking the desired reference value.
- Ensure the robustness of the system.
- Generate the input reference current within the fuel cell current limits and dynamics.

2.2.2 Hybrid System Control Design

For the inner loop, one will use the backstepping approach, which consists of designing stabilised controls for non-linear dynamic systems [27, 28]. The system is decomposed into 1st order progressively stabilised subsystems using Lyapunov theory. The process is completed once the control objectives are achieved. The error vector and its derivative are defined by:

$$Z = \begin{pmatrix} z_1 \\ z_2 \\ z_3 \\ z_4 \end{pmatrix} = \begin{pmatrix} L_1(x_1 - x_{1ref}) \\ L_2(x_2 - x_{2ref}) \\ L_3(x_3 - x_{3ref}) \\ C_{dc}(x_4 - x_{4ref}) \end{pmatrix} \Longrightarrow \dot{Z} = \begin{pmatrix} \dot{z}_1 \\ \dot{z}_2 \\ \dot{z}_3 \\ \dot{z}_4 \end{pmatrix} = \begin{pmatrix} L_1(\dot{x}_1 - \dot{x}_{1ref}) \\ L_2(\dot{x}_2 - \dot{x}_{2ref}) \\ L_3(\dot{x}_3 - \dot{x}_{3ref}) \\ C_{dc}(\dot{x}_4 - \dot{x}_{4ref}) \end{pmatrix}$$

One considers the quadratic Lyapunov function and its derivative defined as follows:

$$V = \frac{1}{2} z^T z = \frac{1}{2}(z_1^2 + z_2^2 + z_3^2 + z_4^2) \Longrightarrow \dot{V} = \frac{1}{2}(\dot{z}^T z + z^T \dot{z}) = z_1\dot{z}_1 + z_2\dot{z}_2 + z_3\dot{z}_3 + z_4\dot{z}_4 \quad (14)$$

Consider the positive integers k_1, k_2, k_3, k_4 and choose:

$$\begin{cases} \dot{z}_1 = -k_1 z_1 + z_4 \\ \dot{z}_2 = -k_2 z_2 + z_4 \\ \dot{z}_3 = -k_3 z_3 \\ \dot{z}_4 = -k_4 z_4 - z_1 - z_2 \end{cases} \quad (15)$$

The error vector Z is therefore defined by:

$$\dot{Z} = \begin{pmatrix} \dot{z}_1 \\ \dot{z}_2 \\ \dot{z}_3 \\ \dot{z}_4 \end{pmatrix} = \begin{pmatrix} -k_1 & 0 & 0 & 1 \\ 0 & -k_2 & 0 & 1 \\ 0 & 0 & -k_3 & 0 \\ -1 & -1 & 0 & -k_4 \end{pmatrix} \begin{pmatrix} z_1 \\ z_2 \\ z_3 \\ z_4 \end{pmatrix} = -KZ \quad (16)$$

K is a positive constant synthesis matrix. $\dot{Z} = -KZ$ is a first-order differential equation with constant coefficients whose solution is:

$$Z(t) = Z(0)e^{-Kt} \tag{17}$$

The tracking error Z tends to zero exponentially after a finite time. This time can be minimised by increasing K.

The condition: $\dot{V} = -k_1 z_1^2 - k_2 z_2^2 - k_3 z_3^2 - k_4 z_4^2 < 0$ guarantees the global asymptotic stability of the system.

$$\begin{pmatrix} L_1(\dot{x}_1 - \dot{x}_{1ref}) \\ L_2(\dot{x}_2 - \dot{x}_{2ref}) \\ L_3(\dot{x}_3 - \dot{x}_{3ref}) \end{pmatrix} = \begin{pmatrix} -k_1 z_1 + z_4 \\ -k_2 z_2 + z_4 \\ -k_3 z_3 \end{pmatrix} \tag{18}$$

We replace $\dot{x}_1, \dot{x}_2 \text{and } \dot{x}_3$ by their respective expressions in equation (10), we deduce the different control laws:

$$\begin{cases} u_1 = 1 - \dfrac{1}{x_4}\left(k_1 z_1 - z_4 + V_{FC} - r_1 x_1 - L_1 \dot{I}_{L_{1ref}}\right) \\ u_2 = 1 - \dfrac{1}{x_4}\left(k_2 z_2 - z_4 + V_{FC} - r_2 x_2 - L_2 \dot{I}_{L_{2ref}}\right) \\ u_{34} = \dfrac{1}{x_4}\left(k_3 z_3 + x_5 - (r_3 + r_{SC}) x_3 - L_3 \dot{I}_{SC_{ref}}\right) \end{cases} \tag{19}$$

The control signals μ_3 and μ_4 with respective average values u_3 and u_4 will be generated by adopting the following scheme:

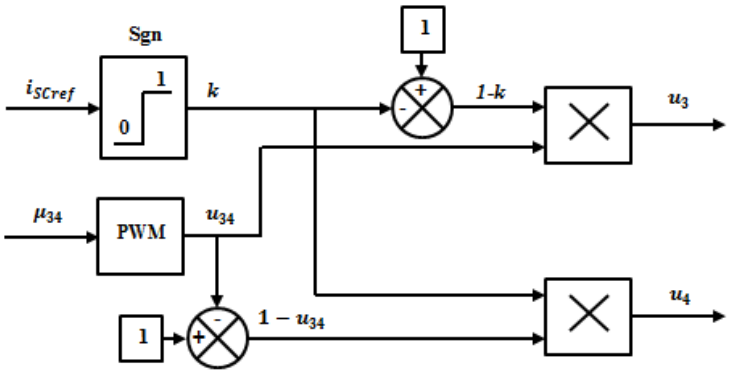

Figure 7. Control Signals u_3 and u_4 Computing Block

2.2.3. Energy Management Flatness Concept

The concept of flatness was introduced by Marquez and Fliess [29]. This concept makes it possible to control the dynamic behaviour of a system using differential algebra formalism.

The selection of this control mode is justified by its capability to manage system trajectories and transient behaviours analytically. This approach offers several notable advantages:

- Analytical Expression: State and control variables can be expressed directly through the selected flat outputs, bypassing the need to solve differential equations.

- Reference Calculation: It allows for using calculated reference values rather than measured ones, which reduces the impact of measurement noise on the control signals.
- Robust Performance: The flatness-based control approach exhibits excellent robustness to variations and uncertainties in system parameters.

The main benefit of this strategy is its ability to plan the trajectory of flatness output. By defining this trajectory, the evolution of state variables and control parameters can be anticipated without solving differential equations. This also ensures that the system's dynamic constraints, such as current and power limits, are adhered to by carefully selecting the reference trajectory for the flat outputs.

2.2.3.1. Trajectory Planning

The fuel cell and super-capacitors currents are assumed to be regulated and to follow their references. They can be expressed by:

$$\begin{cases} i_{FC} = I_{FCref} = \dfrac{P_{FC}}{V_{FC}} = \dfrac{P_{FCref}}{V_{FC}} \\ i_{SC} = I_{SCref} = \dfrac{P_{SC}}{V_{SC}} = \dfrac{P_{SCref}}{V_{SC}} \end{cases} \tag{20}$$

where P_{FC} and P_{SC} are the fuel cell and super-capacitor powers, respectively.

The DC bus and super-capacitors storage energies are denoted, respectively. y_{dc} and y_{SC} are defined by:

$$\begin{cases} y_{dc} = \dfrac{1}{2} C_{dc} V_{dc}^2 \\ y_{sc} = \dfrac{1}{2} C_{sc} V_{sc}^2 \end{cases} \tag{21}$$

The power balance at the common DC bus is given by:

$$P_{FC} + P_{SC} - p_{FC} - p_{SC} - V_{dc} i_{dc} - \dot{y}_{dc} = 0 \tag{22}$$

The energy vector (composed of the flat outputs), the state vector and the control vector are respectively defined by:

$$\begin{cases} Y = [y_{dc} \quad y_T]^T = [y_1 \quad y_2]^T \\ \chi = [V_{dc} \quad V_{SC}]^T = [x_4 \quad x_5]^T \\ \Upsilon = [P_{SCref} \quad P_{PACref}]^T = [\upsilon_1 \quad \upsilon_2]^T \end{cases}$$

where: $y_T = y_{dc} + y_{sc}$.

Using the equation (21), one can express the state variables. (x_4, x_5) as a function of the flat outputs y_1 and y_2 :

$$\begin{cases} x_4 = V_{dc} = \sqrt{\dfrac{2y_{dc}}{C_1}} = \sqrt{\dfrac{2y_1}{C_1}} \\ x_5 = V_{SC} = \sqrt{\dfrac{2y_{SC}}{C_{SC}}} = \sqrt{\dfrac{2(y_T - y_{dc})}{C_{SC}}} = \sqrt{\dfrac{2(y_2 - y_1)}{C_{SC}}} \end{cases} \quad (23)$$

Using the equations (20-22), the controls v_1 and v_2 can be expressed as a function of the flat outputs considered:

$$\begin{cases} v_1 = 2P_{SCmax}\left[1 - \sqrt{1 - \left(\dfrac{\dot{y}_1 + \sqrt{\frac{2y_1}{C_{dc}}}\, i_{dc} - P_{FC_{dc}}}{P_{SCmax}}\right)}\right] \\ v_2 = 2P_{FCmax}\left[1 - \sqrt{1 - \left(\dfrac{\dot{y}_2 + \sqrt{\frac{2y_1}{C_{dc}}}\, i_{dc}}{P_{FCmax}}\right)}\right] \end{cases} \quad (24)$$

Where:

$$\begin{cases} P_{SCmax} = \dfrac{V_{SC}^2}{4r_{SC}} \\ P_{FCmax} = \dfrac{V_{FC}^2}{4r_{FC}} \end{cases} \quad (25)$$

Therefore, one can conclude that the system is flat since the state and control variables are expressed in terms of the flat outputs considered.

2.2.3.2. Development of Energy Control Laws

Since the system is never perfectly known, open-loop control often leads to the appearance of a static error on the controlled variable. To ensure that the energies. y_{dc} and y_T are controlled at their reference trajectories y_{dcref} and y_{Tref}, one will need to fix the dynamics of the errors. The control laws governing the evolution of the energy errors $(y_{dcref} - y_{dc})$ and $(y_{Tref} - y_T)$ and allowing them to converge 0 are given by:

$$\begin{cases} (\dot{y}_{dcref} - \dot{y}_{dc}) + k_{1p}(y_{dcref} - y_{dc}) + k_{1i}\int (y_{dcref} - y_{dc})dt = 0 \\ (\dot{y}_{Tref} - \dot{y}_T) + k_{2p}(y_{Tref} - y_T) + k_{2i}\int (y_{Tref} - y_T)dt = 0 \end{cases} \Rightarrow \begin{cases} \dot{\varepsilon}_{dc} + k_{1p}\varepsilon_{dc} + k_{1i}\int \varepsilon_{dc}dt = 0 \\ \dot{\varepsilon}_T + k_{2p}\varepsilon_T + k_{2i}\int \varepsilon_T dt = 0 \end{cases} \quad (26)$$

From these equations, one can deduce:

$$\begin{cases} \dot{y}_1 = \dot{y}_{dc} = \dot{y}_{dcref} + k_{1p}(y_{dcref} - y_{dc}) + k_{1i}\int (y_{dcref} - y_{dc})dt \\ \dot{y}_2 = \dot{y}_T = \dot{y}_{Tref} + k_{2p}(y_{Tref} - y_T) + k_{2i}\int (y_{Tref} - y_T)dt \end{cases} \quad (27)$$

In Laplace notation, those expressions become:

$$\begin{cases} s^2 + k_{1p}s + k_{1i} = 0 \\ s^2 + k_{2p}s + k_{2i} = 0 \end{cases} \quad (28)$$

Identifying with the standard expression for a second order, one deduces:

$$\begin{cases} (k_{1p}, k_{1i}) = (2\xi_1\omega_{1n}, \omega_{1n}^2) \\ (k_{2p}, k_{2i}) = (2\xi_2\omega_{2n}, \omega_{2n}^2) \end{cases} \quad (29)$$

Where: (ξ_1, ξ_2) are the damping coefficients, and $(\omega_{1n}, \omega_{2n})$ the natural pulsations.

The parameters k_{1p}, k_{2p}, k_{1i} and k_{2i} must be chosen strictly positive to ensure the system's asymptotic stability. The choice of pulses depends on the dynamics of the system components: PEMFC, super-capacitors and DC bus.

The fuel cell is characterised by slow dynamics, which must be compensated for using the storage device constituted by the super-capacitors, which have faster dynamics. Based on the dynamic classification of sources and load, the energy management strategy aims to ensure that each power source is used optimally.

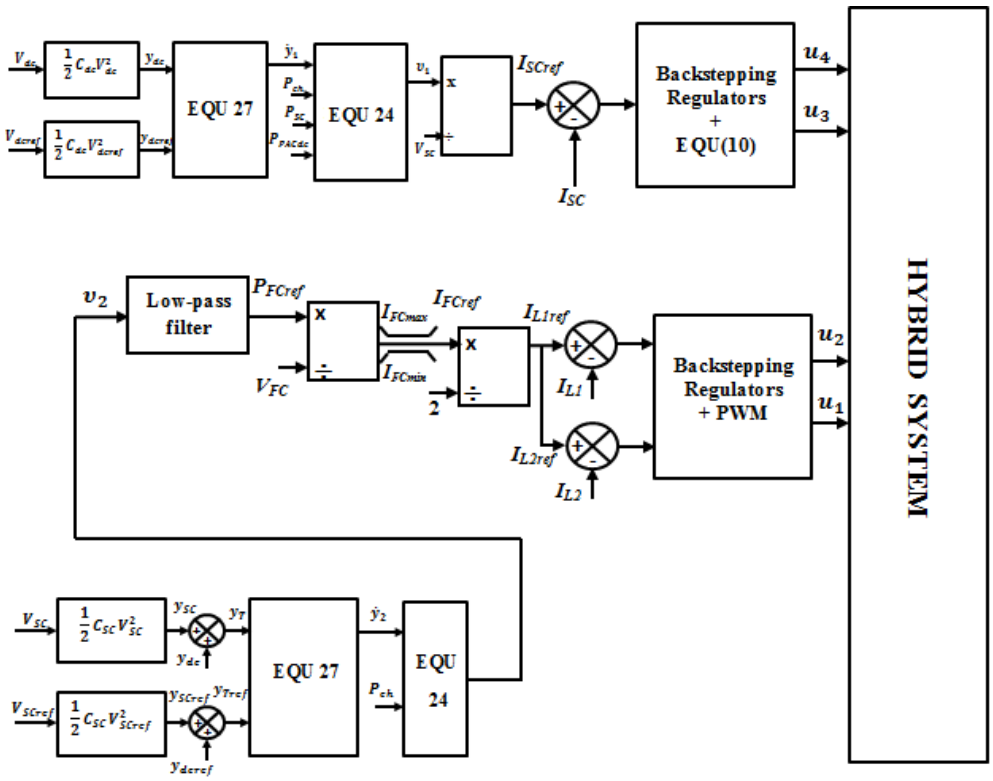

Figure 8. Detailed diagram of hybrid system control strategies

The following inequalities can, therefore, be written:

$$\omega_{FC} \text{"} \omega_{2n} \text{"} \omega_{1n} \text{"} \omega_d \quad (30)$$

Where: ω_{FC}, ω_{2n}, $\omega_{1n}$and ω_d are respectively the switching pulsation of the PEMFC filter, the natural pulsation of the super-capacitor energy regulator, the natural pulsation of the DC bus energy regulator and the sampling pulsation $(\omega_d = 2\pi f_d)$.

Once the flat outputs are stabilised, the whole system becomes exponentially stable because all the variables in the system are expressed as a function of these flat outputs. To account for the dynamics of the PEMFC, one uses a second-order low-pass filter of the form:

$$F_{FC}(s) = \frac{1}{\frac{s^2}{\omega_{FC}^2} + \frac{2\xi_{FC}}{\omega_{FC}} s + 1} \tag{31}$$

Figure 8 shows a detailed diagram of the hybrid system's control strategies.

3. Results and Discussions

The hybrid system converter was simulated using SimPower of Matlab-Simulink software with the set of parameter values in Tables 2 and 3 to verify the theoretical results predicted in the second section.

Table 2. Hybrid system components values

Converter Type	**Inter Leaved Boost Converter**	**Buck-Boost Converter**
Inductances values	$L_1 = L_2 = 10\text{mH}$	$L_3 = 0{,}5\mu\text{H}$
Resistors values	$r_1 = r_2 = 0{,}15\Omega$	$r_2 = 0{,}2\Omega$
Capacitors values	$C_{dc} = 3\mu\text{F}$	$C_{SC} = 140\mu\text{F}$

Table 3. Controllers' parameters values and fuel cell characteristics

PEMFC	$\boldsymbol{\xi_{PAC} = 1}$ $\boldsymbol{\omega_{PAC} = 0{,}5\text{rd/s}}$
Backstepping Controller	$k_1 = k_2 = 8000$ $k_3 = k_4 = 9000$
Flatness Concept	$\xi_1 = \xi_2 = 0{,}7$ $\omega_{1n} = 300\text{rd/s}$ $\omega_{2n} = 200\text{rd/s}$ $k_{1p} = 420\text{rd/s}$ $k_{2p} = 280\text{rd/s}$ $k_{1i} = 4.10^4\text{rd}^2/\text{s}^2$ $k_{2i} = 9.10^4\text{rd}^2/\text{s}^2$

In this section, one will simulate the behaviour of the hybrid system in response to different desired power levels. The results generated using MATLAB will be employed to validate both the system model and the proposed control strategies for managing energy flows.

One will start by validating the energy management of the system through the examination of three distinct operating modes:

- Mode 1 : $P_{load} < P_{FCmin}$.
- Mode 2 : $P_{FCmin} \leq P_{load} \leq P_{FCmax}$.
- Mode 3 : $P_{load} > P_{FCmax}$

To assess the performance of the differential flatness-based controller in managing the DC bus energy using fuel cell and SC, simulations using the Matlab/SimPower tool were carried out by modifying the desired power. The obtained results are shown in Figure 9.

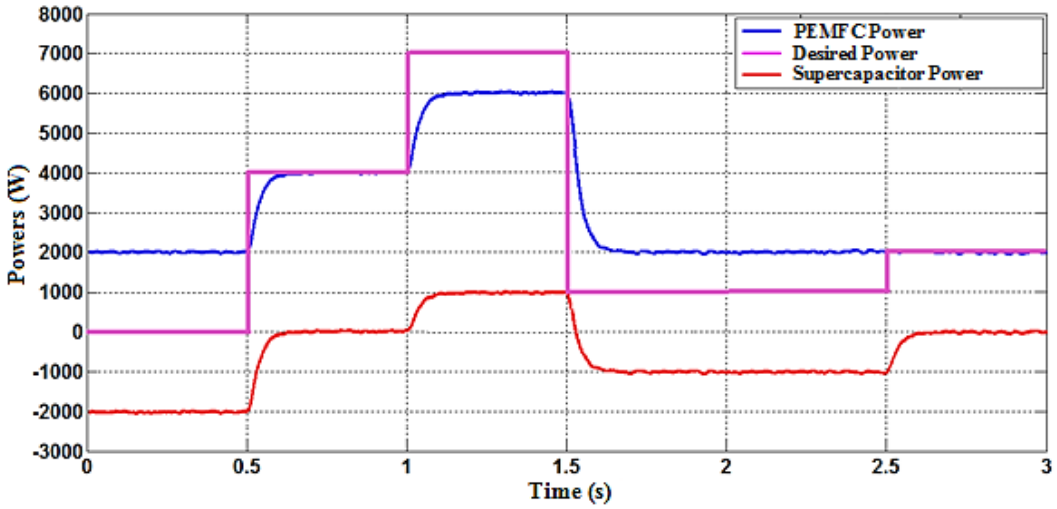

Figure 9. Graph representing the different powers involved

- At the beginning ($t = 0s$) and in the absence of power demand (stop mode), the fuel cell operates at its minimum power of $2000W$. This energy is ultimately stored in the super-capacitors, which are in recovery mode.
- At $t = 0{,}5s$ the power demand rises to $4000W$. This power is entirely provided by the fuel cell. Simultaneously, the power of the SCs decreases to zero (discharge mode).
- Afterwards, at $t = 1s$, the desired power increases to $7000W$. The fuel cell can supply a maximum of $6000W$, so the SCs provide an additional $1000W$ to meet the total demand (discharge mode).
- At $t = 1{,}5s$, the requested power drops to $1000W$. The fuel cell reduces its power from $6000W$ to $2000W$, maintaining its minimum level. The SCs, which transition from discharge to charge mode absorb the excess power.
- Finally, at $t = 2{,}5s$, the desired power increases slightly to $2000W$. The fuel cell continues to operate at its minimum power of $2000W$, while the SCs discharge to balance the system, reaching $0W$.

It can be stated that energy management utilising the flatness concept in conjunction with the backstepping approach yields positive results, with simulations validating the theoretical findings. The flatness-based algorithm enhances system reliability by effectively controlling power flow and managing energy. This combination proves to be theoretically sound and demonstrates practical effectiveness in improving system performance through simulation results.

This hybrid power management strategy effectively maintains energy balance while optimising the contributions from fuel cells and super-capacitors. By dynamically adjusting power outputs based on changing demands, the system ensures stable and efficient operation, showcasing the benefits of integrating these energy storage technologies within a hybrid network. The different signals illustrating the dynamic behaviour of the hybrid system are presented in Figure 10.

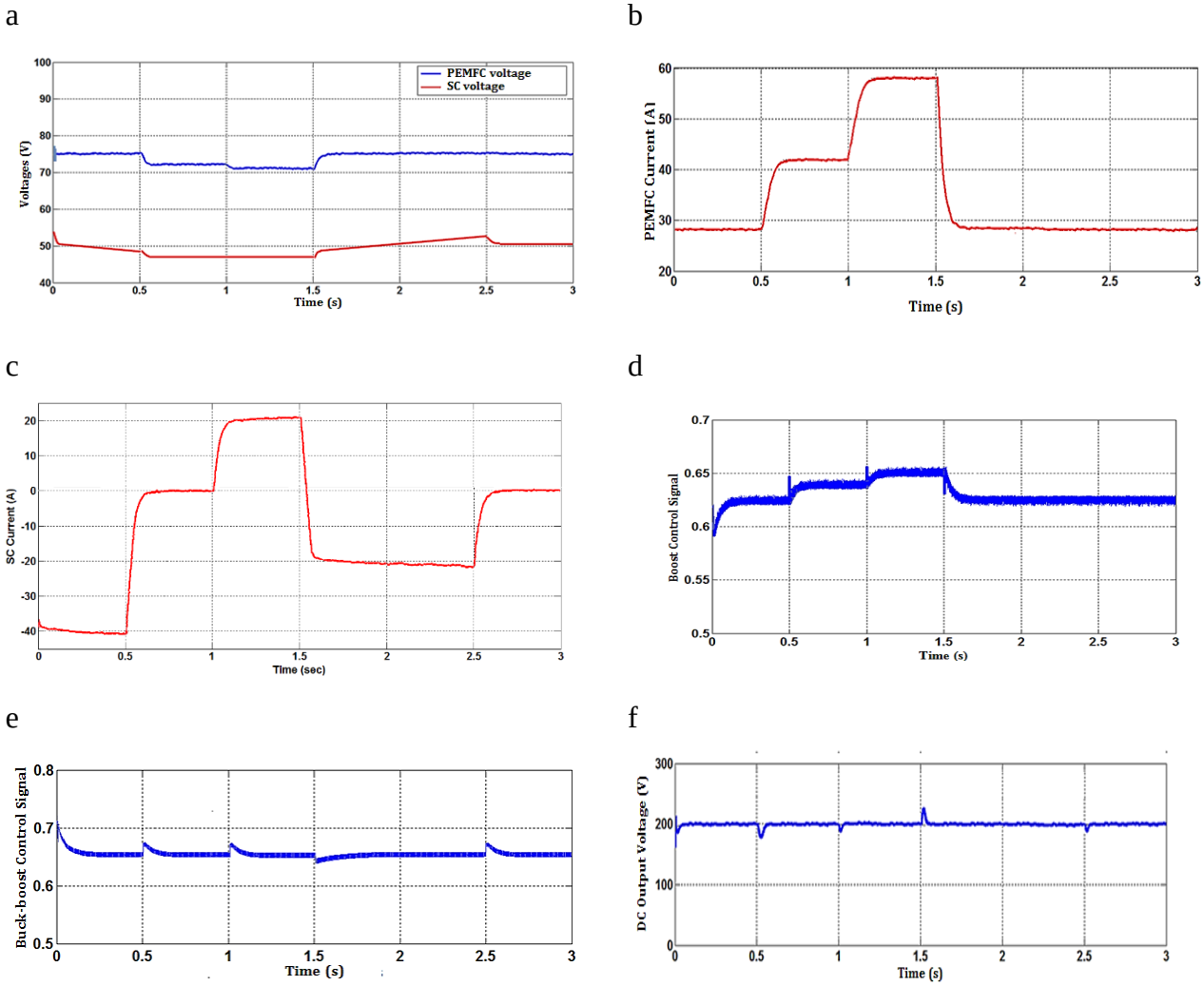

Figure 10. (a) PEMFC and SC Voltages; (b) PEMFC Current ; (c) SC Current; (d) Boost Control Signal; (e) Buck-Boost Control Signal; (f) Output DC Voltage

- Figure 10-a illustrates the voltage curves of the PEMFC and SC. The voltage of the PEMFC exhibits minimal variation, which supports the decision to restrict its power output. The SC voltage, depending on its state (charge or discharge), varies around the reference, which is practically defined by:

$$V_{SCref} = \frac{\sqrt{V_{SCmax}^2 + V_{SCmin}^2}}{2} \approx 50V.$$

- Figures 10-b and 10-c display the currents for the PEMFC and the super-capacitors, respectively. Both currents are maintained within the limits specified by the design requirements.

- The various switch control signals are shown in Figures 10-d (for the interleaved boost converter) and 10-e (for the buck-boost converter). Both signals justify the duty cycle values already calculated.
- Figure 10-f shows the output voltage. One remarks that it tracks its reference very well.

In summary, the hybrid system uses a fuel cell combined with the super-capacitors. Hybridisation of the fuel cell is necessary to improve its lifetime, expand the system's overall efficiency, and reduce the stresses to which it is subjected.

The multivariable control of the PEMFC-SC hybrid system is based on the flatness concept combined with the backstepping approach. The control laws for the DC and total bus energies consist of generating the SC and PEMFC power references.

The power generation required from the PEMFC must be limited in scope to consider the dynamic constraints of the fuel cell. This is achieved by using a second-order low-pass filter to which the transfer function is linear.

The recovered power is used to deduce the reference current. I_{FCref} which must respect the limits of the PEMFC in the interval $[I_{FCmin}, I_{FCmax}]$.

Platitude control of the hybrid system's power flow and energy management has increased its reliability. Finally, the super-capacitors play a crucial role in recovering excess energy and returning it when necessary, optimising overall energy management.

4. Conclusions

This research explores effective energy management in a hybrid system combining fuel cells and super-capacitors, employing the flatness concept alongside the backstepping approach. The simulations validate the theoretical framework, revealing significant system reliability and performance improvements.

Key findings demonstrate the system's capability to maintain energy balance and optimise contributions from both energy sources, ensuring stable operation under varying demand conditions. The control strategies effectively manage power flow, which illustrates the voltages and currents of the PEMFC and super-capacitors.

The fuel cell's power output is limited to enhance efficiency and extend its lifespan, while super-capacitors recover excess energy for optimal management. This research highlights the practical benefits of these advanced control strategies in renewable energy applications, showcasing the potential of hybrid systems to provide reliable, autonomous solutions in remote environments and contribute to sustainable energy demands.

Declaration of Competing Interest: The authors declare they have no known competing interests.

References

[1] P. Fragiacomo, F. Piraino, M. Genovese, O. Corigliano, and G. De Lorenzo, "Strategic overview on fuel cell-based systems for mobility and electrolytic cells for hydrogen production," *Procedia Computer Science,* vol. 200, pp. 1254-1263, 2022, doi: https://doi.org/10.1016/j.procs.2022.01.326.

[2] M. Menner and G. Reichert, "EU hydrogen strategy," 2020.

[3] O. Bethoux, "Hydrogen fuel cell road vehicles: state of the art and perspectives," *Energies,* vol. 13, no. 21, p. 5843, 2020, doi: https://doi.org/10.3390/en13215843.

[4] T. Chinese, F. Ustolin, B. Marmiroli, H. Amenitsch, and R. Taccani, "Experimental analysis on the influence of operating profiles on high temperature polymer electrolyte membrane fuel cells," *Energies,* vol. 14, no. 20, p. 6737, 2021, doi: https://doi.org/10.3390/en14206737.

[5] W. Wang, F. Qu, W. Li, G. Wang, and F. Zeng, "Modeling and simulation analysis of a typical fuel cell vehicle," in *2021 IEEE 5th Information Technology, Networking, Electronic and Automation Control Conference (ITNEC)*, 2021, vol. 5: IEEE, pp. 877-883, doi: https://doi.org/10.1109/itnec52019.2021.9587080.

[6] A. Loskutov, A. Kurkin, A. Shalukho, I. Lipuzhin, and R. Bedretdinov, "Investigation of PEM Fuel Cell Characteristics in Steady and Dynamic Operation Modes," *Energies,* vol. 15, no. 19, p. 6863, 2022, doi: https://doi.org/10.3390/en15196863.

[7] K. Al-Hamed and I. Dincer, "A novel integrated solid-oxide fuel cell powering system for clean rail applications," *Energy Conversion and Management,* vol. 205, p. 112327, 2020, doi: https://doi.org/10.1016/j.enconman.2019.112327.

[8] O. Corigliano, G. De Lorenzo, and P. Fragiacomo, "Preliminary design of AR/SOFC cogeneration energy system using livestock waste," *Procedia Computer Science,* vol. 180, pp. 935-942, 2021, doi: https://doi.org/10.1016/j.procs.2021.01.344.

[9] S. Ma *et al.*, "Fuel cell-battery hybrid systems for mobility and off-grid applications: A review," *Renewable and Sustainable Energy Reviews,* vol. 135, p. 110119, 2021, doi: https://doi.org/10.1016/j.rser.2020.110119.

[10] D. Devadiga, M. Selvakumar, P. Shetty, and M. S. Santosh, "The integration of flexible dye-sensitised solar cells and storage devices towards wearable self-charging power systems: A review," *Renewable and Sustainable Energy Reviews,* vol. 159, p. 112252, 2022, doi: https://doi.org/10.1016/j.rser.2022.112252.

[11] H. Moradisizkoohi, N. Elsayad, and O. A. Mohammed, "Experimental verification of a double-input soft-switched DC–DC converter for fuel cell electric vehicle with hybrid energy storage system," *IEEE Transactions on Industry Applications,* vol. 55, no. 6, pp. 6451-6465, 2019, doi: https://doi.org/10.1109/tia.2019.2937288.

[12] K. Gaouzi, H. El Fadil, O. Benzouina, Z. El Idrissi, A. Rachid, and F. Giri, "Discrete-time constrained control of the fuel cell association with buck-boost dc-dc power converter with continuous input," *IFAC-PapersOnLine,* vol. 55, no. 12, pp. 288-293, 2022, doi: https://doi.org/10.1016/j.ifacol.2022.07.326.

[13] Z. El Idrissi, H. El Fadil, F. Belhaj, A. Lassioui, K. Gaouzi, and I. Bentalhik, "Real-time implementation of adaptive non-linear control of Buck-Boost DC-DC power converter with a continuous input current for fuel cell energy sources," *IFAC-PapersOnLine,* vol. 55, no. 12, pp. 420-425, 2022, doi: https://doi.org/10.1016/j.ifacol.2022.07.348.

[14] R. Majdoul, A. Touati, A. Ouchatti, A. Taouni, and E. Abdelmounim, "Comparison of backstepping, sliding mode and PID regulators for a voltage inverter," *International Journal of Electrical and Computer Engineering (IJECE),* vol. 12, no. 1, pp. 166-178, 2022, doi: https://doi.org/10.11591/ijece.v12i1.pp166-178.

[15] A. Souissi, "Adaptive sliding mode control of a PEM fuel cell system based on the super twisting algorithm," *Energy Reports,* vol. 7, pp. 3390-3399, 2021, doi: https://doi.org/10.1016/j.egyr.2021.05.069.

[16] M. Ahmed, A. Elhassane, and A. Mohamed, "Modelling and Passivity-based Control of a Non Isolated DC-DC Converter in a Fuel Cell System," *IAES Int. J. Rob. Autom.(IJRA),* vol. 7, no. 3, p. 197, 2018, doi:

https://doi.org/10.11591/ijra.v7i3.pp197-204.

[17] B. Yodwong, P. Thounthong, D. Guilbert, and N. Bizon, "Differential flatness-based cascade energy/current control of battery/super-capacitor hybrid source for modern e–vehicle applications," *Mathematics*, vol. 8, no. 5, p. 704, 2020, doi: https://doi.org/10.3390/math8050704.

[18] M. Bougrine, A. Benalia, E. Delaleau, and M. Benbouzid, "Minimum time current controller design for two-interleaved bidirectional converter: Application to hybrid fuel cell/super-capacitor vehicles," *international journal of hydrogen energy*, vol. 43, no. 25, pp. 11593-11605, 2018, doi: https://doi.org/10.1016/j.ijhydene.2017.07.188.

[19] P. Thounthong *et al.*, "Differential flatness based-control strategy of a two-port bidirectional super-capacitor converter for hydrogen mobility applications," *Energies*, vol. 13, no. 11, p. 2794, 2020, doi: https://doi.org/10.3390/en13112794.

[20] A. Siangsanoh *et al.*, "Series hybrid fuel cell/super-capacitor power source," *Mathematics and Computers in Simulation*, vol. 184, pp. 21-40, 2021, doi: https://doi.org/10.1016/j.matcom.2020.02.001.

[21] H. F. Ghavidel and S. M. Mousavi-G, "Modeling analysis, control, and type-2 fuzzy energy management strategy of hybrid fuel cell-battery-supercapacitor systems," *Journal of Energy Storage*, vol. 51, p. 104456, 2022, doi: https://doi.org/10.1016/j.est.2022.104456.

[22] X. Tian, R. He, and Y. Xu, "Design of an energy management strategy for a parallel hybrid electric bus based on an IDP-ANFIS scheme," *IEEE access*, vol. 6, pp. 23806-23819, 2018, doi: https://doi.org/10.1109/access.2018.2829701.

[23] Q. Li, X. Meng, F. Gao, G. Zhang, W. Chen, and K. Rajashekara, "Reinforcement learning energy management for fuel cell hybrid systems: A review," *IEEE Industrial Electronics Magazine*, vol. 17, no. 4, pp. 45-54, 2022, doi: https://doi.org/10.1109/mie.2022.3148568.

[24] V. Mounica and Y. Obulesu, "Hybrid power management strategy with fuel cell, battery, and super-capacitor for fuel economy in hybrid electric vehicle application," *Energies*, vol. 15, no. 12, p. 4185, 2022, doi: https://doi.org/10.3390/en15124185.

[25] A. Djerioui *et al.*, "Energy management strategy of super-capacitor/fuel cell energy storage devices for vehicle applications," *International Journal of Hydrogen Energy*, vol. 44, no. 41, pp. 23416-23428, 2019, doi: https://doi.org/10.1016/j.ijhydene.2019.07.060.

[26] J. C. Amphlett, R. Baumert, R. F. Mann, B. A. Peppley, P. R. Roberge, and T. J. Harris, "Performance modeling of the Ballard Mark IV solid polymer electrolyte fuel cell: II. Empirical model development," *Journal of the Electrochemical Society*, vol. 142, no. 1, p. 9, 1995, doi: https://doi.org/10.1149/1.2043959.

[27] Y. Fang and J. Fei, "Adaptive backstepping current control of active power filter using neural compensator," *Mathematical Problems in Engineering*, vol. 2019, no. 1, p. 5130738, 2019, doi: https://doi.org/10.1155/2019/5130738.

[28] Z. Hekss *et al.*, "Advanced non-linear controller of single-phase shunt active power filter interfacing solar photovoltaic source and electrical power grid," *International Transactions on Electrical Energy Systems*, vol. 31, no. 12, p. e13237, 2021, doi: https://doi.org/10.1002/2050-7038.13237.

[29] R. Marquez and M. Fliess, "Linear predictive control revisited: a flatness based approach," in *1999 European Control Conference (ECC)*, 1999: IEEE, pp. 3214-3219, doi: https://doi.org/10.23919/ecc.1999.7099822.